

RNAi-Mediated Targeting of Noncoding and Coding Sequences in DNA Repair Gene Messages Efficiently Radiosensitizes Human Tumor Cells

Zhiming Zheng^{1,2}, Wooi Loon Ng², Xiangming Zhang², Jeffrey J. Olson³, Chunhai Hao⁴, Walter J. Curran², and Ya Wang²

Abstract

Human tumor cell death during radiotherapy is caused mainly by ionizing radiation (IR)-induced DNA double-strand breaks (DSB), which are repaired by either homologous recombination repair (HRR) or nonhomologous end-joining (NHEJ). Although siRNA-mediated knockdown of DNA DSB repair genes can sensitize tumor cells to IR, this approach is limited by inefficiencies of gene silencing. In this study, we show that combining an artificial miRNA (amiR) engineered to target 3'-untranslated regions of XRCC2 (an HRR factor) or XRCC4 (an NHEJ factor) along with an siRNA to target the gene coding region can improve silencing efficiencies to achieve more robust radiosensitization than a single approach alone. Mechanistically, the combinatorial knockdown decreased targeted gene expression through both a reduction in mRNA stability and a blockade to mRNA translation. Together, our findings establish a general method of gene silencing that is more efficient and particularly suited for suppressing genes that are difficult to downregulate by amiR- or siRNA-based methods alone. *Cancer Res*; 72(5); 1–8. ©2012 AACR.

Introduction

Radiotherapy, one of the leading approaches in cancer therapy, contributes to more than 50% of cancer treatment. Ionizing radiation (IR) kills tumor cells mainly by inducing DNA double-strand breaks (DSB) and, therefore, results in cell reproductive death (loss of the capacity to sustain proliferation; refs. 1, 2). Therefore, inhibiting DNA DSB repair is an efficient way to sensitize human cells to IR-induced killing. In mammalian cells, there are two pathways to repair DNA DSB: homologous recombination repair (HRR) and nonhomologous end-joining (NHEJ). XRCC4 is an essential factor that stimulates DNA ligase IV in the NHEJ pathway (3, 4), and XRCC2 is an essential factor in the HRR pathway (5, 6). Targeting the *XRCC4* coding region with siRNA has been reported to manipulate the NHEJ pathway (7) and targeting the *XRCC2* coding region with siRNA has been reported to affect the HRR pathway (8). Many human tumors have a strong DNA DSB repair capacity; therefore, discovering a new approach that could target DNA repair genes more efficiently is essential to

maximally sensitize human tumor cells to IR-induced killing.

miRNAs are evolutionally conserved noncoding RNA with 19 to 23 nucleotide that negatively regulate gene expression by binding to the 3'-untranslated region (UTR) of target genes (9, 10). It has been shown that the artificial miRNA (amiR) could be used for silencing gene expression by targeting its 3'-UTR (11). We were interested in testing the hypothesis that combining amiR to target the 3'-UTR of the DNA repair gene and siRNA to target the coding sequence of the same gene could maximally knock down the gene. In this study, we chose *XRCC4* and *XRCC2* as the target genes to test whether we could use the combined approach to maximally knock down the genes and sensitize human tumor cells to IR-induced killing. Our data showed promising results and indicate the feasibility and efficiency of the combined approach for these repair genes. We believe that this combined approach is also very useful for many other gene targeting purposes, especially for some genes that are difficult to target using a single approach (either siRNA or amiR).

Materials and Methods

Human tissues, tumor cell lines, and irradiation

The frozen human brain nontumor tissues and glioblastoma multiforme (GBM) samples were derived from brain surgeries at Emory University, Atlanta, GA. Human brain tumor cell lines (U87MG and T98G) and human lung cancer cell lines (A549 and H1299) were purchased from American Type Culture Collection. A human normal bronchial epithelia cell line, HBEC-3KT, was obtained from the laboratory of Dr. John Minna at the University of Texas Southwestern, Dallas, TX (12). Human

Authors' Affiliations: ¹Department of Neurosurgery, Provincial Hospital affiliated to Shandong University, Shandong University, Jinan, China; and Departments of ²Radiation Oncology, ³Neurosurgery, and ⁴Pathology and Laboratory Medicine, Emory University School of Medicine, Winship Cancer Institute of Emory University, Atlanta, Georgia

Corresponding Author: Ya Wang, Department of Radiation Oncology, Emory University School of Medicine, 1365 Clifton Rd, NE, Atlanta, GA 30322. Phone: 404-778-1832; Fax: 404-778-1750; E-mail: ywang94@emory.edu

doi: 10.1158/0008-5472.CAN-11-2785

©2012 American Association for Cancer Research.

normal astrocyte cells and a brain tumor cell line, LN229, were obtained from the laboratory of Dr. Erwin Van Meir at Emory University (13). The human nontumor cell lines, HBEC-3KT and LN229, were cultured as described previously (12, 13) and verified by a soft agar colony-forming assay. IR was carried out with an X-ray machine (X-RAD 320, N. Branford 320 kV, 10 mA, the filtration with 2-mm aluminum) in our laboratory. The dose rates were about 2 Gy/min.

Construction of amiR-expressing plasmid

The *XRCC4*- or *XRCC2*-specific amiR was designed by a BLOCK-iT RNAi Designer tool and purchased from Invitrogen. A BLAST analysis was conducted to avoid the designed sequence with substantial homology to other genes. The primers are shown in the Supplementary Table S1. The double-strand oligonucleotides were generated by annealing equal amounts of each single-strand oligonucleotide and cloned into a pcDNA6.2-GW/EmGFP-miR vector. After the sequence was verified, the amiR expression clone was inserted into the destination vector pLenti6/V5-DEST (Invitrogen) according to the manufacturer's instructions.

Lentivirus packaging and infection

These experiments were similar to that described previously (14, 15). Briefly, approximately 4×10^6 293FT cells were seeded in a 100-mm dish overnight. The pLenti6/V5-GW/miR expression plasmid Control-amiR, amiR-*XRCC4*, or amiR-*XRCC2* with ViraPower Packaging Mix (Invitrogen) were formed into a complex with Lipofectamine 2000 (Invitrogen) and transfected into the 293FT cells. The media containing the DNA-Lipofectamine 2000 complexes were removed and replaced with complete culture medium. The virus containing supernatant was collected and supplemented with polybrene. The mixture was added to the cell cultures. The transduced cells were harvested after 72- to 96-hour postinfection for further experiments. Some cells were treated with blasticidin and selected for amiR stably expressed cells.

siRNA and mimic amiR transfection

The control RNA and siRNA pool against human *XRCC4* or *XRCC2* were purchased from Santa Cruz Biotechnology Inc. The amiR mimic and single siRNA against human *XRCC4* or *XRCC2* were purchased from Qiagen. The sequence of siRNA against human *XRCC4* (Catalogue no. # SI00051905) is UUCUA-CUUGGUGCAAUAUCAGtt (for sense) and CUGAUUUGCAC-CAAGUAGAAtt (for antisense). The sequence of siRNA against human *XRCC2* (Catalogue no. # SI00077091) is UUAUAGUUU-GUGUCGUUGCAAAtt (for sense) and UUGCAACGACACAAA-CUAUAAtt (for antisense). U87MG and A549 cells were grown to 30–50% confluence, and RNA transfections were carried out with Lipofectamine 2000 (Invitrogen) according to the manufacturer's instructions. The transfection efficiency for the cells was checked by a Western blotting assay at different times after transfection.

Quantitative real-time PCR

Total small RNA in the human tumor cells were extracted by a Qiazol kit (Qiagen). RNA (1 μ g) was used to synthesize

cDNA by using a SuperScript III kit (Invitrogen) according to the manufacturer's instructions. Real-time PCR was carried out on a SDS 7500 Fast Instrument (Applied Biosystems) with the System Software version 2.0.5 following the default cycling protocol (at 95°C for 10 minutes, followed by 40 cycles of 95°C for 15 seconds, and 60°C for 1 minute). Fluorescence readings were taken during the 60°C step. Primers (Supplementary Table S1) for *XRCC4*, *XRCC2*, or β -actin (an endogenous control) mRNA were designed with Primer Express 3.0 software (Applied Biosystems). Relative quantities were calculated with the $\Delta\Delta C_t$ method. Quantitative real-time PCR was carried out at least 3 times, and a no-template control was included as a negative control.

Luciferase assay

Similar to the methods as described in our previous studies (14, 15), 293FT cells were transfected with the plasmids (encoding the 3'-UTR of *XRCC2* or *XRCC4* containing the potential amiR-binding site or the site was deleted) with or without 100 nmol/L amiR mimics (Qiagen) in 48-well plates. The primers used for the experiments are listed in the Supplementary Table S2. The cells were harvested 48 hours after transfection. The cells were then lysed with a luciferase assay kit (Promega) according to the manufacturer's protocol and were measured on a luminescence microplate reader LUMIstar Galaxy (BMG lab-technologies). β -galactosidase or *Renilla* luciferase was used for normalization.

Western blotting

Whole-cell lysates for Western blotting were prepared as described previously (14, 15). The antibodies against *XRCC4*, *XRCC2*, and β -actin were purchased from Santa Cruz Biotechnology. The antibodies against *XRCC4*, *XRCC2*, and β -Actin were purchased from Santa Cruz Biotechnology Inc. and incubated overnight at 4°C. The membrane was scanned and analyzed using an Odyssey Infrared Imaging System (LI-COR Biosciences).

γ -H2AX foci assay

The assay followed the previously reported protocol (16, 17) with some modifications. Briefly, cells were fixed in 4% paraformaldehyde for 15 minutes, permeabilized for 5 minutes on ice in 0.2% Triton X-100, and blocked in 10% normal goat serum. The coverslips were incubated with an anti- γ -H2AX antibody (Millipore) for 1 hour, washed in PBS, 1% BSA, and incubated with an Alexa Fluor 488-conjugated goat anti-mouse secondary antibody (Invitrogen) for 1 hour at room temperature. Cells were washed in PBS and mounted by using Vectashield-mounting medium with 4',6-diamidino-2-phenylindole (DAPI; Vector Laboratories). Fluorescent images were captured by using a CarlZeiss Axio Scope A1 with an Epi-Fluorescence microscope (Germany) equipped with an MRm Cooled Digital Camera with Axiovision software (version 4.8) for camera control, image acquisition, processing, and a module for multichannel display.

Clonogenic surviving assay

Cellular sensitivity to radiation was determined by the loss of colony-forming ability as described previously (14, 15). Briefly, 2×10^5 cells were plated, per 60-mm dish with 3 mL of medium. The cells were irradiated 48 hours later. The cells were then collected and plated, aiming at 20 to 200 colonies per dish. Two replicates were prepared for each datum point and were incubated for 2 weeks to allow colonies to develop. Colonies were stained with crystal violet (100% methanol solution) before counting.

Results

XRCC2 or XRCC4 expressed higher in human tumor tissues/cells than in human nontumor tissues/cells

To study the effects of knocking down the DNA repair gene *XRCC2* (for the HRR pathway) or *XRCC4* (for the NHEJ pathway) for the sensitization of human tumor cells to radiation, we were interested in knowing the different expression of the repair genes in human normal tissues/cells and human tumor tissues/cells as such information would allow us to evaluate whether the sensitization approach could particularly benefit from killing more tumor cells. For this purpose, we compared the expression levels of *XRCC2* or *XRCC4* in the human GBM or lung tumor cell lines and their nontumor counterparts by using Western blot analysis. The results showed that when compared with the human normal astrocyte cells (Fig. 1A, lane 1), the human GBM cell lines (Fig. 1A, lane 2–4) showed higher levels of *XRCC2* or *XRCC4*, particularly in the U87MG cells (Fig. 1A,

lane 2). Similar to the GBM cell line results, when compared with the human normal bronchial epithelial cell cells (Fig. 1A, lane 5), the human lung cancer cell lines (Fig. 1A, lane 5 and 6) showed higher levels of *XRCC2* or *XRCC4*, particularly in the A549 cells (Fig. 1A, lane 5). We then compared the expression levels of *XRCC2* or *XRCC4* in the frozen human GBM tissues and human nontumor tissues by using a real-time PCR assay. The results also showed higher expression levels of *XRCC2* or *XRCC4* in the human GBM tissues than in their nontumor counterpart tissues (Fig. 1B). These data suggest that it might be common that these repair genes highly express in human tumors and, therefore, knocking down these genes could be particularly beneficial for the tumor radiosensitization. On the basis of these data, we chose U87MG (human GBM cell line) and A549 (human lung cancer cell line) cells in our following experiments because the levels of *XRCC2* and *XRCC4* were relatively higher in these 2 cell lines (framed lanes in Fig. 1A) when compared with the normal human cells and other human brain and lung tumor cell lines tested. After choosing the candidate genes and cell lines, we designed the amiR that targets *XRCC2* or *XRCC4* and examined the effects of the amiR on knocking down the targeted genes because siRNA is a relatively mature approach for knocking down a gene.

The amiR against *XRCC4* or *XRCC2* efficiently inhibited the targeted gene expression

Natural mammalian miRNA only requires 6 to 8 seed nucleotides to match the sequence of the targeted gene 3'-UTR, therefore, one miRNA could target multiple mRNAs. To avoid the nonspecific effects, we decided to choose the completely matched strategy (the amiR completely matched the target sequence). On the basis of the sequence of *XRCC2* or *XRCC4* 3'-UTR, we identified the potential-targeted sequences of 3'-UTR that could be bound by an amiR (Fig. 2A). On the basis of the information, we designed the construct encoding the precursor of amiR against *XRCC4* or *XRCC2* (Fig. 2B) and inserted the sequences into a lentiviral vector as we described previously (14, 15). To examine whether the sequence in the 3'-UTR of *XRCC2* or *XRCC4* could be bound by the amiR, we conducted the luciferase assay. The results showed that the amiR could bind well to the targeted sequence (Fig. 2C), suggesting the amiR could work as a miRNA to decrease the targeted gene expression. We then infected the plasmid encoding amiR-*XRCC2*, amiR-*XRCC4*, or both into U87MG or A549 cells. After using the antibiotic selection for 10 generations, we obtained the stable amiR expressed cells that showed the positive GFP signals that reflected the amiR expression frequency of more than 80% (Fig. 3A). We next examined the levels of the targeted protein *XRCC2* and *XRCC4* in these cells. The results showed that the miRs efficiently reduced their targeted gene expression in both U87MG and A549 cells (Fig. 3B), indicating that our designed amiRs worked well even in cells that were coinfecting with the 2 vectors (Fig. 3B). After we obtained the stable amiR expressed cells, we examined the effects of the amiR on the proliferation (by growth curve) and clonogenic rate (plating efficiency) in these cells without any treatment. The results showed that when compared with noninfected cells and the vector alone-infected cells, the

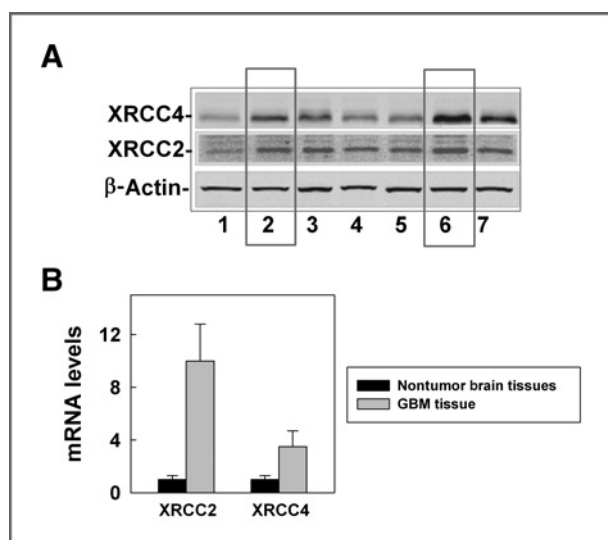


Figure 1. XRCC2 and XRCC4 are highly expressed in human tumor cell lines and tissues. A, the XRCC2 and XRCC4 levels were detected in different human tumor cell lines by Western blotting. 1, normal human astrocyte cells; 2, U87MG cells; 3, T98G cells; 4, LN229 cells; 5, normal human bronchial epithelial cells: HBEC-3KT cells; 6, A549 cells; and 7, H1299 cells. The frames represent that the U87MG and A549 cells were chosen for the following experiments described in this study. B, the *XRCC2* or *XRCC4* mRNA levels were detected in 3 samples from different human nontumor brain tissues and 5 samples from different GBMs by real-time PCR with the specific primers (Supplementary Table S1).

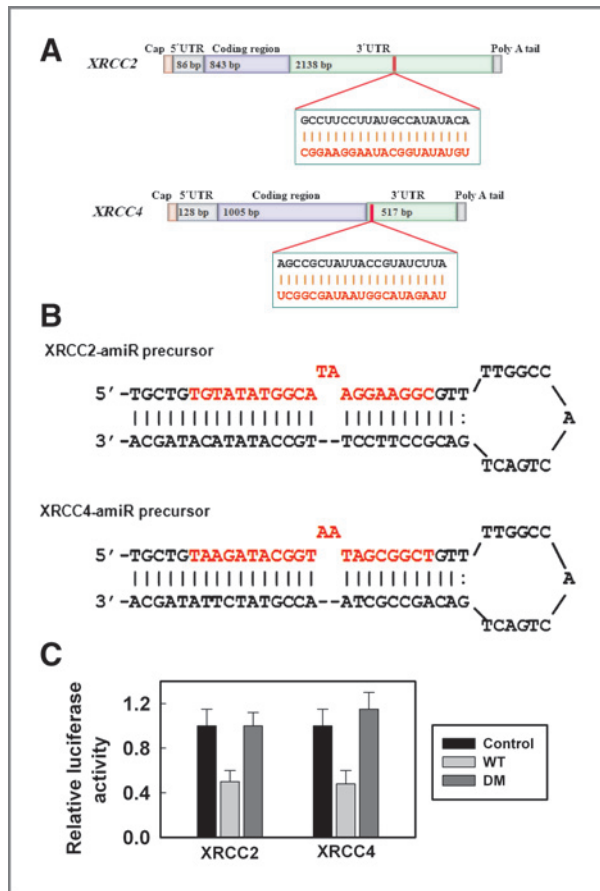


Figure 2. Design of the amiR targeting *XRCC2* or *XRCC4*. A, the targeted sequence in the 3'-UTR of *XRCC2* or *XRCC4* gene: the total nucleotide number in different regions of the *XRCC2* or *XRCC4* was indicated. The targeting sequence of the *XRCC2* by the amiR starts from the nucleotide 1,052 of the 3'-UTR, and the targeting sequence of the *XRCC4* by the amiR starts from nucleotide 85 of the 3'-UTR. The sequence in black represents the 3'-UTRs and the red represents the amiRs. B, precursor-amiR (pre-amiR) double-strand oligonucleotides: the pre-amiR against *XRCC2* or *XRCC4* was designed by the BLOCK-IT RNAi Designer tool and purchased from Invitrogen. The sequence was cloned into a pcDNA6.2-GW/EmGFP-miR vector as described in Materials and Methods. C, the effects of the amiR-binding site in the 3'-UTR of *XRCC2* or *XRCC4* on the luciferase activity: 293T cells were transfected with a firefly luciferase reporter plasmid containing partial 3'-UTR of *XRCC2* or *XRCC4* with the putative amiR-binding site (WT) or without the binding site (DM). Luciferase activity was assayed 48 hours after transfection with the amiR mimic (amiR-m) or without the mimic (with a control RNA).

vector encoding amiR-infected cells showed similar proliferation (Supplementary Fig. S1A) and clonogenic rates (Supplementary Fig. S1B), indicating that the amiR expression alone had less toxicity. In addition, when the cells were subcultured for a relatively long time, the target genes were still inhibited (Supplementary Fig. S2A) and the cells still showed more sensitivity to IR-induced killing than their vector alone-infected cells (Supplementary Fig. S2B). These results suggest that although a lower level of the DNA repair gene does not affect normal survival of the cells, it does radiosensitize the cells.

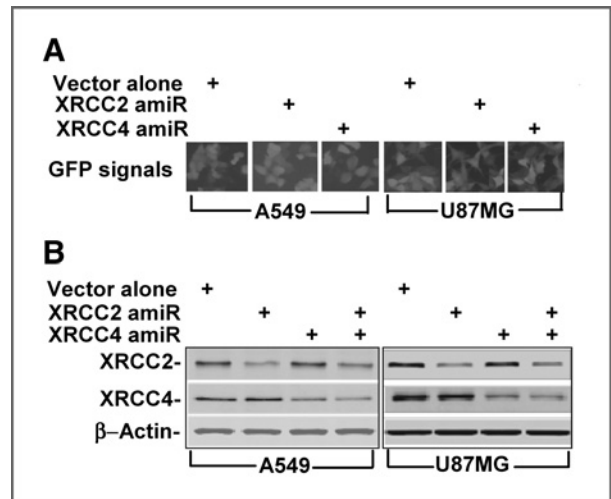
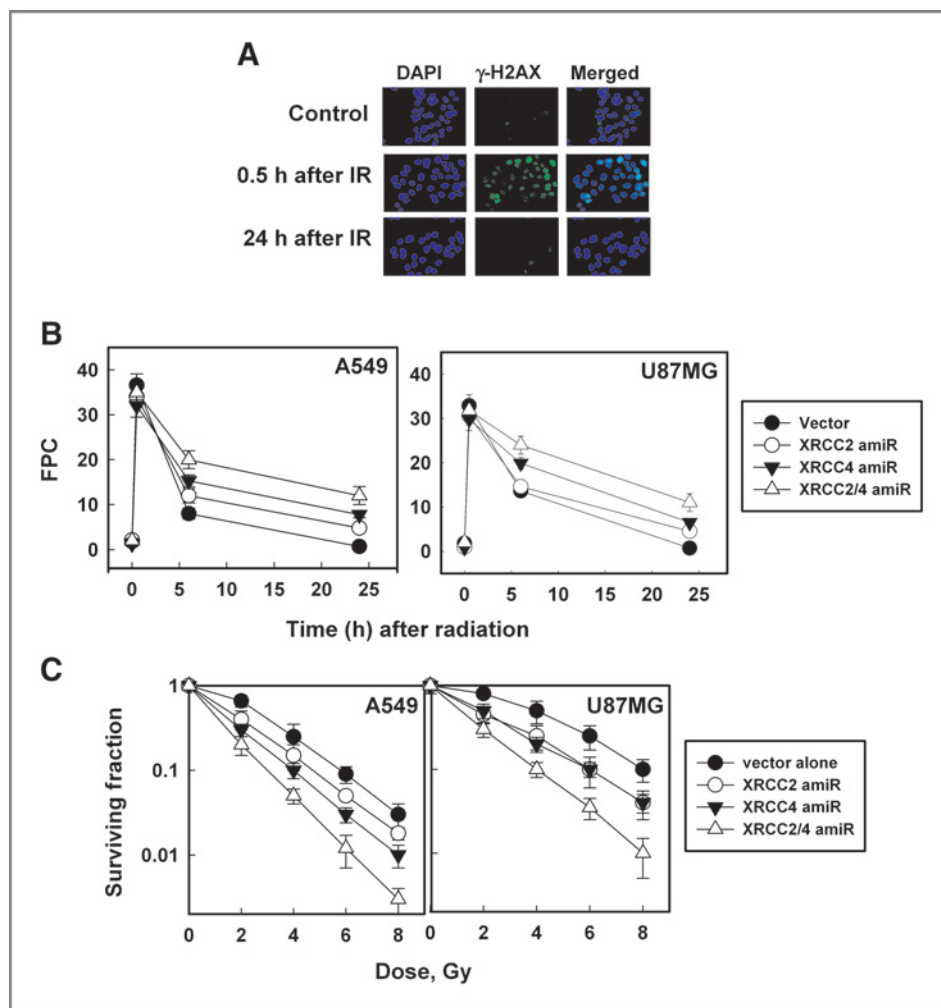


Figure 3. The amiR against *XRCC2* or *XRCC4* decreased the targeted gene expression level. A, detection of the amiR infection efficiency in U87MG and A549 cells. The images reflect GFP signals, which represent the infection efficiencies of the lentivirus vectors. B, the effects of amiR on *XRCC2* or *XRCC4* expression in U87MG and A549 cells. β -Actin was used as an internal loading control.

The amiR against *XRCC4* or *XRCC2* efficiently sensitized human tumor cells to IR-induced killing

Next, we examined the effects of the amiR on the radiosensitization of the cells. We used a γ -H2AX assay to examine the DNA DSB repair efficiency because the signals of γ -H2AX reflect the amounts of DNA DSBs in irradiated cells (16, 18) and indirectly describe the efficiency of DNA DSB repair (17). The results showed that there was no apparent difference in the γ -H2AX-positive ratios among the examined cells immediately after IR (30 minutes), suggesting that there was not much difference in the induction of DNA DSB in these irradiated cells, however, the γ -H2AX-positive ratios clearly increased in the irradiated cells expressing amiR-*XRCC2* or amiR-*XRCC4* when compared with the irradiated cells transfected with the vector alone (Fig. 4A and B). The γ -H2AX-positive ratios left even more in the irradiated cells expressing both amiR-*XRCC2* and amiR-*XRCC4* than in the irradiated cells expressing amiR-*XRCC2* or amiR-*XRCC4* alone (Fig. 4A and B). These results indicate the amiRs inhibited the DNA DSB repair, which is further supported by the survival data (by a clonogenic assay to examine the reproductive death). The results showed that IR killed more cells expressing either amiR-*XRCC4* or amiR-*XRCC2* than the cells expressing the vector alone and killed even more of the cells expressing both amiR-*XRCC2* and amiR-*XRCC4* than the cells expressing amiR-*XRCC2* or amiR-*XRCC4* alone (Fig. 4C). These results show that the amiRs could be used to target DNA repair genes in human tumor cells and sensitize these tumor cells to IR-induced killing. Next, we were interested in detecting the effects of siRNA when targeting the same gene in the tumor cells expressed with the amiR and studying whether the combination approach could enhance the gene knock down efficiency and the human tumor cell radiosensitization.

Figure 4. The amiR targeting the 3'-UTR of the *XRCC2* or *XRCC4* sensitized human tumor cells to IR-induced killing. **A**, incidence of γ -H2AX foci in irradiated U87MG cells. Cells were irradiated with 2 Gy, incubated at 37°C at different times and then processed for γ -H2AX foci counting. Values are the average numbers of γ -H2AX foci per cell (FPC), 50 cells were counted for each slide. **B**, the effect of the amiR on γ -H2AX foci A549 and U87MG cells at different times after 2 Gy exposure. Error bars, SDs. **C**, the effects of the amiR on A549 and U87MG cell radiosensitivity. The clonogenic assay was conducted as described in Materials and Methods. Data shown are the mean and SE from 3 independent experiments.



Combining amiR and siRNA to target *XRCC2* or *XRCC4* more efficiently knocked down the gene and radiosensitized the human tumor cells

To find a better time for gene targeting, we examined the *XRCC2* or *XRCC4* levels in U87MG or A549 cells expressed with the amiR-*XRCC2* or amiR-*XRCC4* at different times after the cells were treated with siRNA against *XRCC2* or *XRCC4*. The results showed that the control RNA did not affect the targeted gene expression at all time points but the siRNA maximally inhibited the targeted gene at 72 hours after transfection in these tumor cells and inhibited more *XRCC2* or *XRCC4* expression in A549 or U87MG cells stably expressed with the amiR (against *XRCC2* or *XRCC4*; Fig. 5A). These results indicate that the combined approach is more efficient than the siRNA or amiR approach alone. We then examined the sensitivities of the combined approach on cell radiosensitivity. The results showed that the cell sensitivity levels depended on the *XRCC2* or *XRCC4* level: the siRNA against *XRCC2* or *XRCC4* more efficiently sensitized A549 or U87MG cells expressing the amiR-*XRCC2* or amiR-*XRCC4* than the cells containing the vector alone (Fig. 5B). These results further show that the combined approach is more efficient than the siRNA or amiR approach alone.

Knocking down *XRCC2* or *XRCC4* by combining small RNAs to target both the coding region and the 3'-UTR through increasing the mRNA degradation and inhibiting the translation

Some commercially available siRNA pools (for targeting a small gene that contains a short coding region) include a small RNA that targets the 3'UTR of the gene. The small RNA that targets the 3'UTR of the gene looks like a miRNA mimic and is a stable double-strand RNA with approximately 22 nucleotides. However, there are no commercially available siRNA pools that include small RNAs to target 3'-UTR of *XRCC2* or *XRCC4*. Also, there is no report to compare the efficiency of any such combined approach (targeting both the coding region and the 3'-UTR of a gene) with the single approach (targeting coding region or 3'-UTR of a gene) on knocking down a gene. In addition, there is no mechanism study for elucidating the advantage of the combined approach if it does have some advantages on the gene knock down. Therefore, we next investigated the effects of the small RNA combined approach (targeting both noncoding and coding regions of *XRCC2* or *XRCC4*) by mixing the amiR mimic and siRNAs against *XRCC2* or *XRCC4*. We also tried to elucidate how the targeted gene

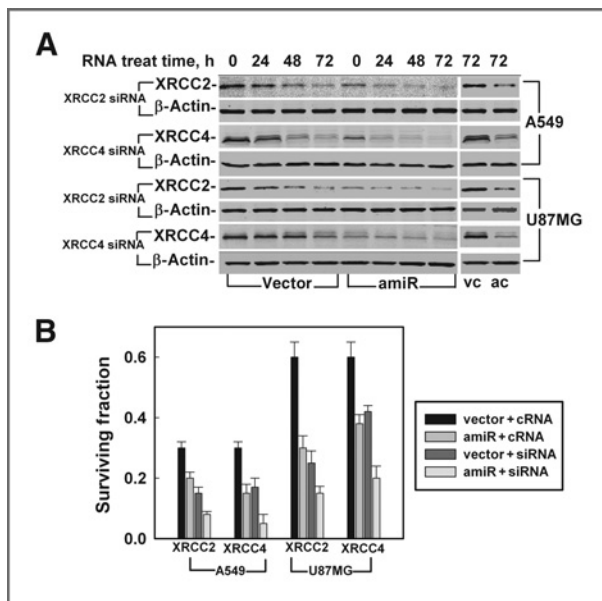


Figure 5. Combining amiR and siRNA to target both the 3'-UTR and coding region of *XRCC2* or *XRCC4* efficiently inhibited the targeted gene and sensitized the human tumor cells to IR-induced killing. **A**, the Western blotting results showed the levels of *XRCC2* or *XRCC4* in A549 or U87MG cells containing amiR or vector alone at different times after transfected with the siRNA. β -Actin was used as an internal loading control. Vector, the cells containing the vector alone; amiR, the cells containing the vector encoding the *XRCC2* or *XRCC4* amiR; vc, the cells containing the vector alone treated with the control RNA; ac, the cells containing the vector encoding the *XRCC2* or *XRCC4* amiR treated with the control RNA. **B**, the effect of siRNA against *XRCC2* or *XRCC4* on sensitizing A549 or U87MG cells containing vector alone or containing vector encoding *XRCC2* or *XRCC4* amiR. The cells were treated with control RNA (cRNA) or siRNA against *XRCC2* or *XRCC4*. At 72 hours after transfection, the cells were exposed to 4 Gy. The cells were collected and plated in new dishes for colony forming as described in Materials and Methods. Data shown are the mean and SE from 3 independent experiments.

was knocked down by the combined approach if the combined approach did show a better effect on knocking down the repair gene than the siRNA or amiR mimic alone. The results showed that an amiR mimic specifically knocked down *XRCC2* or *XRCC4* (Fig. 6A) and mixing it with a siRNA more efficiently decreased the *XRCC2* or *XRCC4* expression level (Fig. 6A). As expected, mixing the amiR mimic with siRNA against *XRCC2* or *XRCC4* more efficiently sensitized the cells to IR-induced killing than using amiR or siRNA against *XRCC2* or *XRCC4* alone (Fig. 6B). These results provide strong evidence that using the small RNAs to target both the noncoding and coding regions of a gene could more efficiently knock down the targeted gene.

Because miRNA could either decrease the mRNA stability or block translation to reduce the targeted gene expression (19, 20), we were interested in elucidating how the amiR mimic decreases the targeted gene expression. For this purpose, we compared the effects of the amiR mimic or/and siRNA on the mRNA level of the targeted gene by using a real-time PCR approach. The results showed that although the protein level of the targeted gene (*XRCC2* or *XRCC4*) between the cells

treated with the amiR mimic and the cells treated with the siRNA did not show any apparent difference (Fig. 6A), the mRNA level of the targeted gene (*XRCC2* or *XRCC4*) was lower in the cells treated with siRNA (~30% of control level) than in the cells treated with amiR mimic (~65% of the control level; Fig. 6C), suggesting that the effects of the amiR on reducing approximately 70% of the protein level of the targeted gene is through both decreasing the mRNA stability (~35%) and blocking translation (~35%). When compared with siRNA alone, combining the amiR and siRNA did not further decrease the mRNA stability (~30%) although the combined approach did further decrease the protein level, suggesting that the additional effect to reduce the protein level by the combined approach is due to the two mechanisms that generate mRNA instability and block translation (Fig. 6C). These results further indicate that the combined approach is specifically

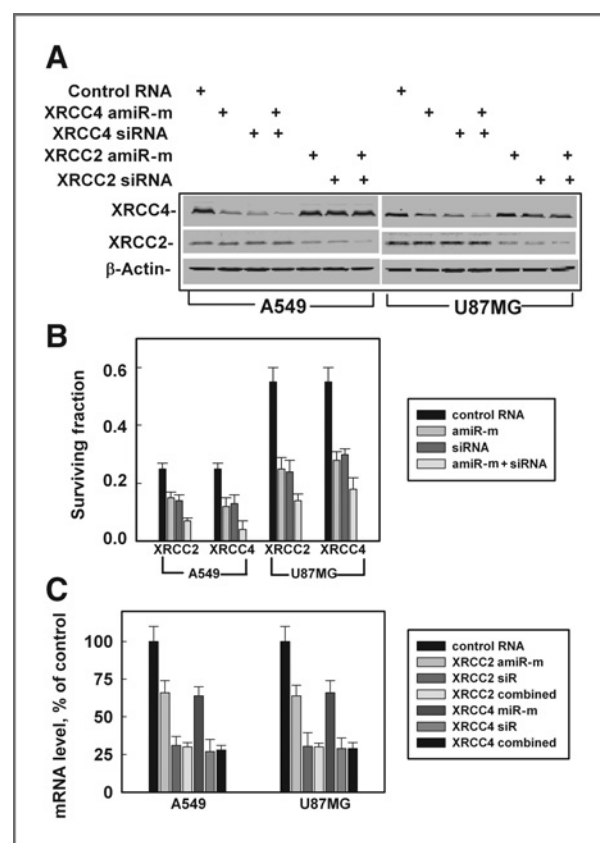


Figure 6. The effects of combining the small RNA (amiR mimic and siRNA) on knocking down the targeted gene and on radiosensitizing the human tumor cells. **A**, the targeted gene expression levels in the cells at 72 hours after transfection with amiR mimic and/or siRNA. The amiR mimic was labeled as amiR-m. β -Actin was used as an internal loading control. **B**, the effect of the combined small RNA (including amiR mimic and siRNA) on cell radiosensitivity. At 72 hours after the small RNA (including amiR mimic and siRNA) transfection, the cells were exposed to 4 Gy and then were collected for colony forming as described in Materials and Methods. Data shown are the mean and SE from 3 independent experiments. **C**, the mRNA levels of *XRCC2* or *XRCC4* in the cells treated with amiR mimic, siRNA, or both were measured by real-time PCR with the proper primers (Supplementary Table S1) as described in Materials and Methods. The independent experiments were done twice with triple samples.

and efficiently for knocking down a gene. Because these small RNAs use different mechanisms to knock down a gene, the combined usage could reach significant additive inhibition of the targeted gene expression.

Discussion

In this study, we show for the first time that our designed amiRs could efficiently knock down DNA repair gene *XRCC2* or *XRCC4*, sensitize human tumor cells to radiation-induced killing, and combining with siRNA could more efficiently knock down the gene and radiosensitize human tumor cells.

A natural miRNA binding to the 3'-UTR of a gene is in a partial complementary manner (21, 22) and one miRNA could target multiple genes (23); so, delivering a miRNA into cells and upregulating the miRNA could result in multiple unexpected effects on the fate of cell. An amiR in a perfect complementary manner, however, could avoid the unexpected side effects by limiting its real target. The results showed that our designed amiRs could efficiently knock down the target genes without affecting the cell growth, suggesting that the amiRs specifically knocked down the target genes. Because most human genes are regulated by miRNA (24), it suggests that most human genes are available to be targeted by a designed amiR. It was reported that the manner of imperfect-complementary binding to 3'-UTR might protect the miRNA from an RNase degradation in *Drosophila* (25), suggesting that the perfect-complementary binding manner (to 3'-UTR of the target gene) of amiRs might affect the stability of the amiRs. To examine the possibility, we designed the *XRCC4* amiRs with imperfect-complementary binding sequences (containing 7 mismatched nucleotides, which is similar to a natural miRNA) to the 3'-UTR (Supplementary Fig. S3A). We transfected the different *XRCC4* amiRs to A549 cells and compared the targeting efficiency as well as the stability of the amiRs. We did not find differences in *XRCC4* knock down efficiency (Supplementary Fig. S3B) or stability of the amiRs (data not shown), suggesting that different from *Drosophila* miRNA stability, the human miRNA stability depends less on the match sequence to a targeted 3'-UTR, which might be due to the relatively short 3'-UTR and a simpler structure of the genome in *Drosophila* when compared with that in humans (26, 27). However, the real mechanism underlying the difference in miRNA degradation between humans and *Drosophila* needs more studies to provide direct evidence. In this study, we found that the efficiency of knocking down the targeted gene dramatically reduced when we mixed an amiR mimic with a siRNA that had more than 5 matched nucleotides (data not shown), suggesting that these small RNAs could interbind each other, and we should avoid the interaction among themselves.

Because NHEJ is a relatively fast process and is not affected by cell-cycle distribution (28, 29), The γ -H2AX-positive ratios in the irradiated cells containing *XRCC4* amiR was higher than that in the irradiated cells containing the vector alone, especially at 6 hours after IR (Fig. 4A and B), indicating the inefficient NHEJ in the cells knocked down with *XRCC4* as NHEJ is a relatively fast process and is not affected by cell-cycle distribution (28, 29). In addition, because HRR is a relatively slow process and occurs only during the S- and G₂ phases (29, 30), the γ -H2AX-positive ratios in irradiated cells containing *XRCC2* amiR was higher than that in the irradiated cells containing the vector alone, especially at 24 hours after IR, indicating the inefficient HRR in the irradiated cells knocked down with *XRCC2*. Interestingly, the radiosensitizing level by the siRNA against *XRCC2* or *XRCC4* in A549 or U87MG cells encoding the amiR *XRCC2* or *XRCC4* reached a similar level in the cells encoding both *XRCC2* and *XRCC4* amiRs (comparing the data shown in Fig. 4C and in Fig. 5B), suggesting that the tumor cell radiosensitization by combining amiR and siRNA to target one repair gene could be comparable by using a single approach (amiR or siRNA) to target 2 repair genes. Efficiently targeting one gene is more important than mildly targeting 2 genes because most human tumor cells are overactivated with one particular DNA repair pathway.

Taken together, our results show for the first time that combining amiR and siRNA to target both the noncoding and coding regions of *XRCC2* or *XRCC4* could more efficiently knock down the DNA DSB repair genes and sensitize human tumor cells to IR-induced killing. We believe that this combined approach will provide a broader use for knocking down any other genes (only if the gene contains more than 100 bp of the 3'-UTR) especially for those genes that are difficult to knock down by using only one approach amiR or siRNA.

Disclosure of Potential Conflicts of Interest

No potential conflicts of interest were disclosed.

Acknowledgments

The authors thank Drs. John Minna and Erwin Van Meir for providing the cell lines and Doreen Theune for editing the manuscript.

Grant Support

This work is supported by NIH grant (GM080771), NASA grant (NNX11AC30G), and Emory Start-up fund (to Y. Wang). Z. Zheng is partially supported by the China Scholarship Council (NO: 2009622099).

The costs of publication of this article were defrayed in part by the payment of page charges. This article must therefore be hereby marked *advertisement* in accordance with 18 U.S.C. Section 1734 solely to indicate this fact.

Received August 16, 2011; revised December 20, 2011; accepted December 26, 2011; published OnlineFirst January 11, 2012.

References

1. Brown JM, Attardi LD. The role of apoptosis in cancer development and treatment response. *Nat Rev Cancer* 2005;5:231-7.
2. Hall E, Giaccia A. *Radiobiology for the radiologist*. 6th ed. Philadelphia, PA: Lippincott Williams & Wilkins; 2005.
3. Grawunder U, Wilm M, Wu X, Kulesza P, Wilson TE, Mann M, et al. Activity of DNA ligase IV stimulated by complex formation with *XRCC4* protein in mammalian cells. *Nature* 1997;388:492-5.
4. Lee KJ, Huang J, Takeda Y, Dynan WS. DNA ligase IV and *XRCC4* form a stable mixed tetramer that functions synergistically with other repair factors in a cell-free end-joining system. *J Biol Chem* 2000;275:34787-96.

5. Liu N, Lamerdin JE, Tebbs RS, Schild D, Tucker JD, Shen MR, et al. XRCC2 and XRCC3, new human Rad51-family members, promote chromosome stability and protect against DNA cross-links and other damages. *Mol Cell* 1998;1:783-93.
6. Johnson RD, Liu N, Jasin M. Mammalian XRCC2 promotes the repair of DNA double-strand breaks by homologous recombination. *Nature* 1999;401:397-9.
7. Bertolini LR, Bertolini M, Anderson GB, Maga EA, Madden KR, Murray JD. Transient depletion of Ku70 and Xrcc4 by RNAi as a means to manipulate the non-homologous end-joining pathway. *J Biotech* 2007;128:246-57.
8. Kondo N, Takahashi A, Mori E, Noda T, Su X, Ohnishi K, et al. DNA ligase IV is a potential molecular target in ACNU sensitivity. *Cancer Sci* 2010;101:1881-5.
9. Esquela-Kerscher A, Slack F. Oncomirs-microRNAs with a role in cancer. *Nat Rev Cancer* 2006;6:259-69.
10. Cho W. OncomiRs: the discovery and progress of microRNAs in cancers. *Mol Cancer* 2007;6:60.
11. Zeng Y, Wagner EJ, Cullen BR. Both natural and designed micro RNAs can inhibit the expression of cognate mRNAs when expressed in human cells. *Mol Cell* 2002;9:1327-33.
12. Ramirez RD, Sheridan S, Girard L, Sato M, Kim Y, Pollack J, et al. Immortalization of human bronchial epithelial cells in the absence of viral oncoproteins. *Cancer Res* 2004;64:9027-34.
13. Kaur B, Cork SM, Sandberg EM, Devi NS, Zhang Z, Klenotic PA, et al. Vasculostatin inhibits intracranial glioma growth and negatively regulates *in vivo* angiogenesis through a CD36-dependent mechanism. *Cancer Res* 2009;69:1212-20.
14. Yan D, Ng1 W, Zhang X, Wang P, Zhang Z, Mo Y, et al. Targeting DNA-PKcs and ATM with miR-101 sensitizes tumors to radiation. *PLoS One* 2010 Jul 1;5:e11397.
15. Ng W, Yan D, Zhang X, Mo Y, Wang Y. Over expression of miR-100 is responsible for the low expression of ATM in the human glioma cell line: MO59J. *DNA Repair* 2010;9:1170-5.
16. Rogakou EP, Pilch DR, Orr AH, Ivanova VS, Bonner WM. DNA Double-stranded breaks induce histone H2AX phosphorylation on serine 139. *J Biol Chem* 1998;273:5858-68.
17. Rothkamm K, Lobrich M. Evidence for a lack of DNA double-strand break repair in human cells exposed to very low x-ray doses. *Proc Natl Acad Sci U S A* 2003;100:5057-62.
18. Redon1 C, Nakamura A, Gouliava K, Rahman A, Blakely W, Bonner W. The Use of Gamma-H2AX as a biodosimeter for total-body radiation exposure in non-human primates. *PLoS One* 2010;5:e15544.
19. Reinhart BJ, Weinstein EG, Rhoades MW, Bartel B, Bartel DP. MicroRNAs in plants. *Genes Dev* 2002;16:1616-26.
20. Hutvagner G, Zamore P. A microRNA in a multiple-turnover RNAi enzyme complex. *Science* 2002;297:2056-60.
21. Jackson RJ, Standart N. How do microRNAs regulate gene expression. *Sci STKE* 2007 Jan 2; 2007(367):re1.
22. Djuranovic S, Nahvi A, Green R. A parsimonious model for gene regulation by miRNAs. *Science* 2011;331:550-3.
23. Griffiths-Jones S, Grocock RJ, van Dongen S, Bateman A, Enright AJ. miRBase: microRNA sequences, targets and gene nomenclature. *Nucleic Acids Res* 2006;34:D140-4.
24. Friedman RC, Farh KK-H, Burge CB, Bartel DP. Most mammalian mRNAs are conserved targets of microRNAs. *Genome Res* 2009;19:92-105.
25. Ameres SL, Horwich MD, Hung J-H, Xu J, Ghildiyal M, Weng Z, et al. Target RNA-directed trimming and tailing of small silencing RNAs. *Science* 2010;328:1534-9.
26. Pesole G, Liuni S, Grillo G, Licciulli F, Mignone F, Gissi C, et al. UTRdb and UTRsite: specialized databases of sequences and functional elements of 5' and 3' untranslated regions of eukaryotic mRNAs. Update 2002. *Nucleic Acids Res* 2002;30:335-40.
27. Mazumder B, Seshadri V, Fox P. Translational control by the 3'-UTR: the ends specify the means. *Trends Biochem Sci* 2003;28:91-8.
28. Metzger L, Iliakis G. Kinetics of DNA double strand breaks throughout the cell cycle as assayed by pulsed field gel electrophoresis in CHO cells. *Int J Radiat Biol* 1991;59:1325-39.
29. Rothkamm K, Kruger I, Thompson LH, Lobrich M. Pathways of DNA double-strand break repair during the mammalian cell cycle. *Mol Cell Biol* 2003;23:5706-15.
30. Takata M, Sasaki MS, Sonoda E, Morrison C, Hashimoto M, Utsumi H, et al. Homologous recombination and non-homologous end-joining pathways of DNA double-strand break. *EMBO J* 1998;17:5497-508.

Cancer Research

The Journal of Cancer Research (1916–1930) | The American Journal of Cancer (1931–1940)

RNAi-Mediated Targeting of Noncoding and Coding Sequences in DNA Repair Gene Messages Efficiently Radiosensitizes Human Tumor Cells

Zhiming Zheng, Wooi Loon Ng, Xiangming Zhang, et al.

Cancer Res Published OnlineFirst January 11, 2012.

Updated version	Access the most recent version of this article at: doi: 10.1158/0008-5472.CAN-11-2785
Supplementary Material	Access the most recent supplemental material at: http://cancerres.aacrjournals.org/content/suppl/2012/01/11/0008-5472.CAN-11-2785.DC1

E-mail alerts [Sign up to receive free email-alerts](#) related to this article or journal.

Reprints and Subscriptions To order reprints of this article or to subscribe to the journal, contact the AACR Publications Department at pubs@aacr.org.

Permissions To request permission to re-use all or part of this article, contact the AACR Publications Department at permissions@aacr.org.